Mineral.Deposita 18,443-455 (1983)

MINERALIUM DEPOSITA

Platinum-group Elements in Rocks from the Voikar-Syninsky Ophiolite Complex, Polar Urals, U.S.S.R.

N. J Page

U.S. Geological Survey, Menlo Park, California

P. J. Aruscavage

U.S. Geological Survey, Reston, Virginia

J. Haffty

U.S. Geological Survey, Denver, Colorado

Analyses of platinum-group elements (PGE) in rocks collected from the Voikar-Syninsky ophiolite in the Polar Urals suggest that the distribution and geochemistry of PGE in this Paleozoic ophiolite are similar to those in Mesozoic ophiolites from elsewhere. Chondrite-normalized PGE patterns for chromitite, the tectonite unit, and ultramafic and mafic cumulate unit have negative slopes. These results are similar to those found for chromitites from other ophiolites; stratiform chromitites show positive slopes. If the magmas that form both types of chromitite originate from similar mantle source material with respect to PGE content, the processes involved must be quite different. However, the distinct chondrite-normalized PGE patterns may reflect differing source materials.

INTRODUCTION

The Voilar-Syninsky ophiolite complex, which lies west of the city of Salekhard in the Polar Urals, U.S.S.R., is an exceptionally well exposed and well preserved ophiolite complex of Paleozoic age. The complex is about 300 km long and 50 to 80 km wide (Fig. 1); it is only moderately serpentinized, is extensively glaciated, and is largely free of vegetation. The area was examined in 10 traverses by participants in an ophiolite conference sponsored by Project 39 of the International Geological Correlation Program in August 1978 (Bogdanov, Morgan, and Page, 1979), during which time samples were collected from the ultramafic tectonite, ultramafic and mafic cumulates, gabbros, and dike rocks in order to investigate the distribution of PGE (platinum-group elements) in the complex. The purposes of this investigation were (1) to document the abundances of PGE in the different parts of an ophiolite, (2) to define the distribution of the PGE with

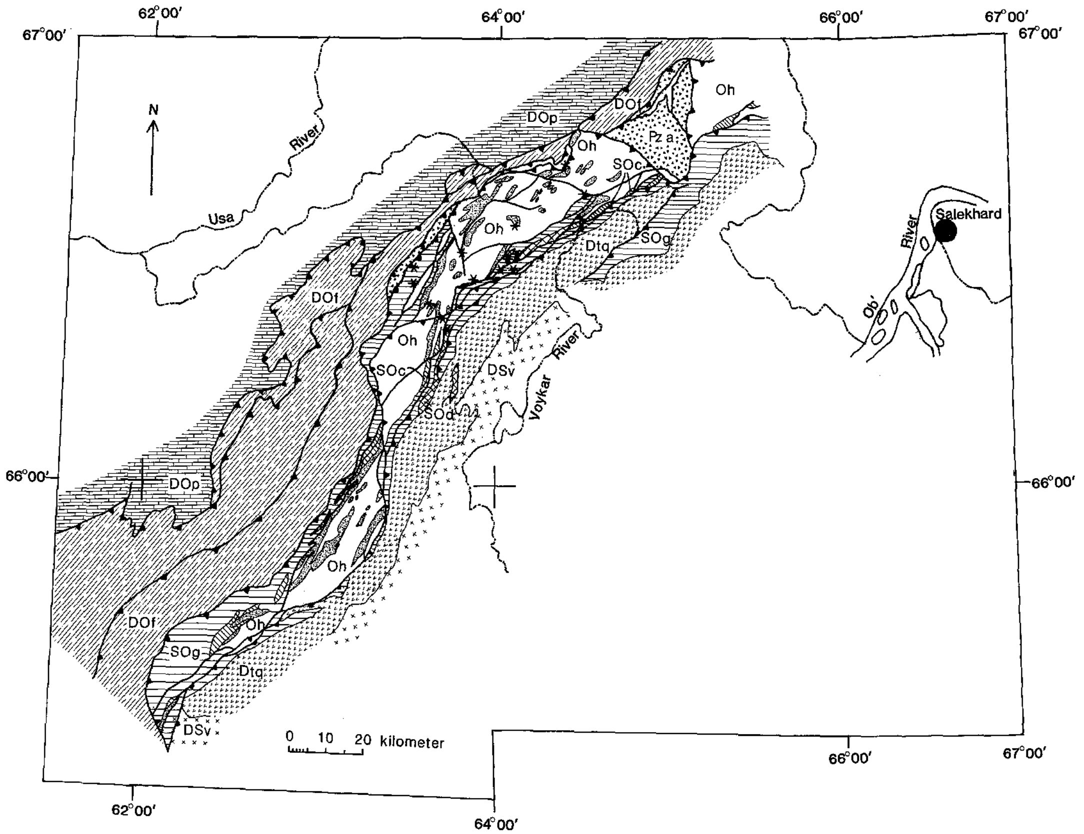

Fig. 1. Geologic sketch map of the Voikar-Syninsky ophiolite complex showing generalized sample locations. Modified from Efimov and others (1978) and Knipper (1979). Stars are sample locations

respect to minor and trace elements, and (3) to compare the PGE geochemistry of a Paleozoic ophiolite with that of Mesozoic ophiolites from various parts of the world.

GEOLOGIC SETTING AND SAMPLE LOCATION

The generalized geology of the Voikar-Syninsky massif consists of thrust slices. From the northwest to southeast they consist of Ordovician to Devonian flyschoid and pleagic sediments, the ophiolite complex, tonalite and diorite, and Silurian and Devonian island-arc sequences, thrust northwestward over an Eocambrian to Paleozoic platform sequence (Fig. 1). The flyschoid and pelagic sediments occur in an imbricate thrust zone in which there are some sedimentary rocks of Upper Mississippian age that contain ophiolite detritus (Bogdanov, Morgan, and Page, 1979). At the eastern margin of the massif, gabbro and diabase dike complexes are intruded and hornfelsed by tonalite that is older than Middle Devonian (K-Ar ages of 375 m.y.; Bogdanov, Morgan, and Page, 1979). Knipper (1979) reported K-Ar ages of 400, 410, 420, and 470 m.y. for gabbroic rocks of the ophiolite. Reviews of the geology, petrology, mineralogy, and structure of the Voikar-Syninsky massif are contained in Efimov and others (1978) and in Sobolev and Dobretsov (1977). More directly focused on the Voikar-Syninsky ophiolite complex are reports by Savel'yev and Savel'yeva (1977) and

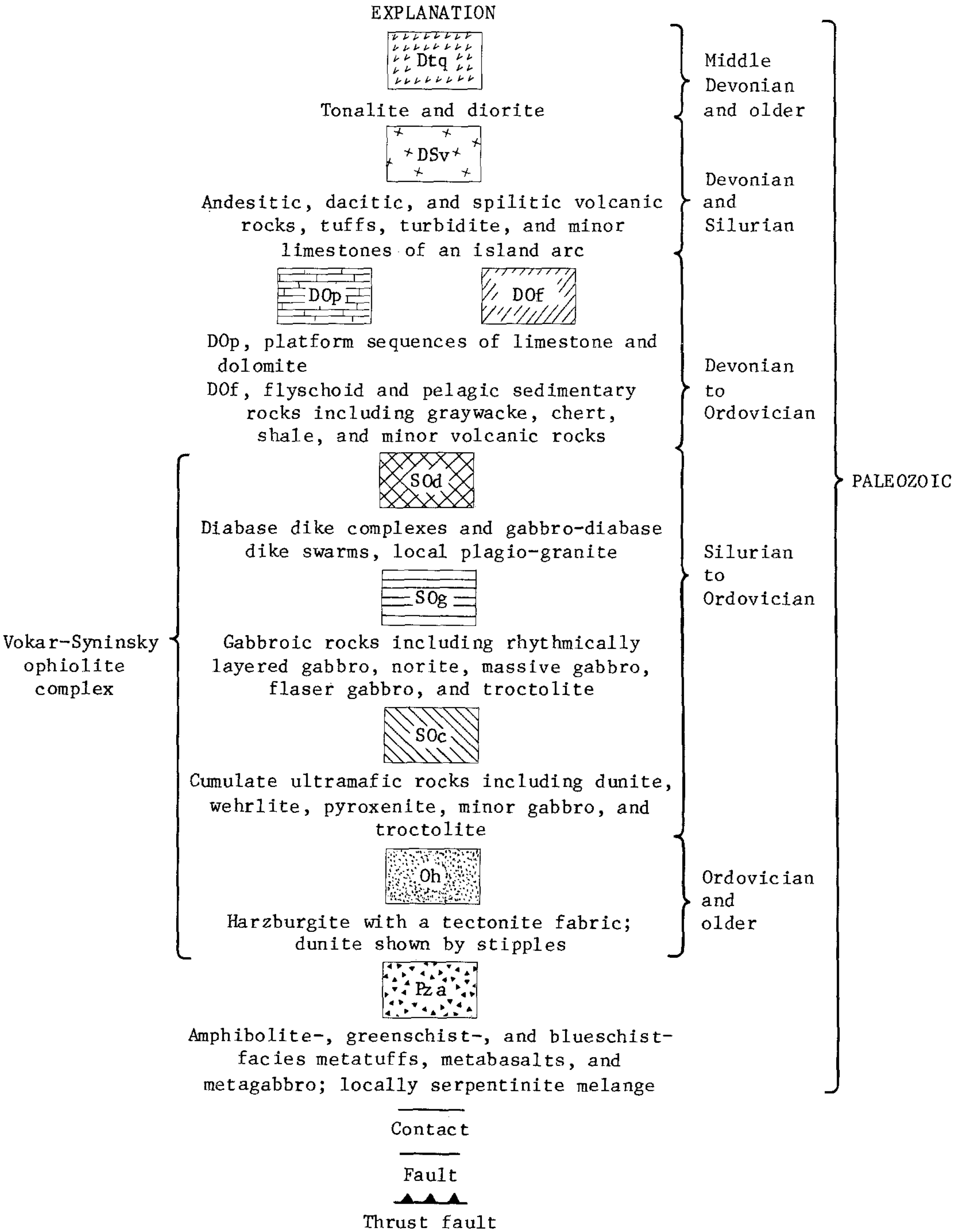

Savel'yeva and Stephanov (1980). The descriptions that follow are based on these references and observations made during the field conference.

Several monoclinal thrust sheets with differing structural and metamorphic histories make up the ophiolite complex. The westernmost sheet contains metagabbro interlayered with metaclinopyroxenite, metawehrlite, and metadunite that have been isoclinally folded, locally sheared, recrystallized, and metamorphosed up to amphibolite grade. The western boundary of this sheet is marked by a fault zone that dips to the southeast and contains slices of basalt, gabbro, tuff, and minor ultramafic rocks metamorphosed to the blueschist and greenschist facies. The eastern boundary is also a southeast-dipping thrust zone that emplaced ultramamfic tectonite over the metagabbro unit. The harzburgite sheet is estimated to be between 4 and 6 km thick (Efimov and others, 1978). Dunite occurs in irregular masses within the harzburgite and is associated with podiform chromitite occurrences. Deformed dunite-harzburgite layering within the central part of the complex defines a broad synform (Savel'yev and Savel'yeva, 1977). Numerous dikes and veins composed of dunite, orthopyroxenite, clinopyroxenite, and websterite cut the harzburgite mass. The eastern contact of the harzburgite is locally a fault but at other places appears to be an unconformity overlain by well-developed, repetitive cumulus sequences of dunite, wehrlite, pyroxenite, and gabbro. The development of slump structures and crossbedding in the layered gabbro and oikocrysts of clinopyroxene in the dunite are evidence that processes similar to those in stratiform intrusions contributed to the development of these layers. Gabbro becomes the dominant rock type in the upper part of the unit and near the top becomes deformed and metamorphosed to amphibolite intruded by dike complexes of diabases. Locally dikes intrude each other and have chilled margins against the dike country rock. Coarse-grained hornblende gabbros and plagiogranite form dikes and irregular pods in the gabbro-diabase dike complex. The eastern margin of the gabbro-diabase dike complex is intruded by the younger tonalite and diorite.

Samples of the ophiolite were collected during 10 traverses described by Efimov and others (1978); general locations are shown in Fig. 1. Sample descriptions and some details of the relations between samples are given in Table 1. Most of the samples were grab samples, apparently representative of the outcrops traversed, that weighed several kilograms.

ANALYTICAL TECHNIQUES AND RESULTS

Analytical information for palladium, platinum, rhodium, iridium, ruthenium, silver, gold, cobalt, chromium, copper, molybdenum, nickel, lead, tin, vanadium, and zinc are included in Table 1. The samples are grouped in the following broad categories: dike complex, gabbroic units, ultramafic and mafic cumulates, and ultramafic tectonite and associated dikes. Individual rock names are based on thin section examination. Platinum, palladium, and rhodium analyses of all samples were performed by a fire-assay-atomic absorption described by Page, Myers and others (1980) and Simon and others (1978) which has detection limits of 0.2, 1.0, 0.1 ppb for Pd, Pt, and Rh, respectively. Some of the samples were also analyzed for palladium, platinum, and rhodium by the method described by Haffty and Riley (1968) using a fire-assay preconcentration step described by Haffty, Riley, and Goss (1977). Palladium, platinum, and rhodium by this method have detection limits of 4, 10, and 5 ppb, respectively. After the fire-assay preconcentration step, iridium and ruthenium were analyzed by the method of Haffty, Haubert, and Page (1980). Detection limits for iridium and ruthenium are 20 and 100 ppb, respectively. The other elements were analyzed by H.J. Calbert and W.B. Crandell by a computerized emission spectrographic technique for silicate rocks for which the relative standard deviation for each reported concentration is plus 50 percent and minus 33 percent.

INTERPRETATION OF THE ANALYTICAL INFORMATION

Within a partially dismembered ophiolite such as the Voikar-Syninsky complex (s. Fig. 1), one of the major problems is to be able to place the rocks into an overall stratigraphic sequence in order to examine geochemical trends or patterns with respect to stratigraphic position. We collected some groups of samples for which we were able to determine the stratigraphic sequence. These include samples sequences 7PU78 to 12PU78, 13PU78 to 17PU78, and 49PU78 to 53PU78. While we have determined the stratigraphy within a group of samples, the field relations did not allow us to determine the relative stratigraphic positions between groups. Because of this difficulty, the data in Table 1 are treated in a general way based on the general sequence: ultramafic tectonite, ultramafic and mafic cumulates, gabbroic units, and dike complex. The highest PGE concentrations in the tectonite unit are Pd, 17 parts per billion (ppb); Pt, 19 ppb; Rh, 5.7 ppb; Ir, 54 ppb; and Ru, 240 ppb. The maximum PGE contents in the ultramafic and mafic cumulates are slightly higher and are Pd, 50 ppb; Pt, 51 ppb; Rh, 48 ppb; Ir, 85 ppb; and Ru, 250 ppb. Maximum PGE contents in the gabbroic and dike units are lower than those in the ultramafic and mafic cumulates. In the gabbroic unit, the largest PGE concentrations found are Pd, 29 ppb; Pt, 24 ppb; Rh, 1.0 ppb; and Ru, 140 ppb.

Arithmetic averages for the PGE values and for other selected elements are different from unit to unit (Table 1); however, examination of the large standard deviations for most of the elements implies that often the differences between the averages for adjacent units are not significant. For example, differences in arithmetic averages for Co between the dike complex and gabbroic units are not significant at a 95-percent confidence level but are significant between gabbroic units and tectonite and associated dike units. The apparent trends of decreasing average concentrations of Co, Cr, Ni, and V and increasing Cu upward in the complex appear to fit differentiation processes. Changes in the PGE content over more limited stratigraphic intervals are not as regular, and definition of trends or patterns is hampered by lack of even more sensitive analytical methods.

Correlations between the PGE and other elements for all of the rocks as a group, for the larger stratigraphic units, and for individual rock types were done by calculating Spearman-rank correlation coefficients and testing their significance. Although there are many interelement correlations with coefficients greater than 0.5 and confidence levels of greater than 95 percent, there are very few correlations of this nature involving the PGE's. Correlations observed include Pt negatively with Yb (-0.68) in a data set of all rocks, negatively with Y (-0.50) and Na (-0.66) in gabbros, and positively with Zr (+0.69) in chromitites; Pd positively with Pt (0.58) in all rocks, with Mn (0.61) in tectonite unit, with Cr (0.65) in gabbros, and with Pt (0.74) in dunite and chromitite; and Rh negatively with Si (-0.69) in tectonites, negatively with Ni (-0.65) and positively with Fe (0.60), Ti (0.66), and Nb (0.65) in chromitite. The correlation coefficients are given in parentheses. The relatively few correlations detected between PGE and other elements that occur in the silicate and oxide minerals suggests that processes which affect silicate and oxides phases affect the PGE differently.

Concentrations of the PGE in individual rock samples and average concentrations for each unit (Table 1), except for the poorly sampled dike complex, were normalized with respect to chondrite concentrations. Data for all of the chromitites were also averaged and calculated as chondrite normalized PGE rations. Chondrite concentrations used in normalizing are Pd, 1,200 ppb; Pt, 1,500 ppb; Rh, 200 ppb; Ru, 1,000 ppb; and Ir, 500 ppb, which are the average values given by McBryde (1972). Figures 2, 3 and 4 show chondrite normalized PGE for individual rocks from the tectonite, ultramafic and mafic cumulate, and gabbroic units, respectively. For many of the samples, the patterns formed by the normalized PGE values are incomplete either because there was not enough sample available for the Ir and Ru analysis or because Ir and Ru were below the levels of detection of the analytical technique used. Nevertheless, there are four groups or types of patterns reflected in the plots of individual rocks; (1) approximately flat patterns, that is

Table 1.--Analyses of the PGE and selected metallic elements for rocks and averages and standard deviations for selected elements for units from the Voikar-Syninsky ophiolite, Polar Urals, U.S.S.R.
[Analysts: Philip J. Aruscavage, Joseph Haffty, and A. W. Haubert for the PGE. H. J. Calbert and W. B. Crandell for the emission spectrographic analyses. tr, trace; H, spectral interference; --, not determined; where two analyses done for Pt, Pd, and Rh, the first one listed is by Aruscavage; the second by Haffty and Haubert; N, arithematic average; (n), number of determinations; , standard deviation. No samples with visible sulfides were used in calculating the average]

Sample number	Pd	Pt	Rh	Ir	Ru	Ag	Au	Co	Cr	Cu	Mo	Ni	Pb	Sn	V	Zn	Rock type	ΣPt+Pd+Rh
	(parts per billion)					(parts per million)												
								DIKE COMPLEX										
6PU78	<0.2	<1.0	<0.1	--	--	<0.1	<10	27	3.3	530	2.8	13	<6.8	1.5	220	87	Hornfels mafic dike with sulfide minerals in contact with tonalite	<
27PU78	0.5	<1.0	<0.1	--	--	<0.1	<10	42	250	42	<1.0	89	<6.8	<1.5	180	51	Plagioclase porhyritic dike	<
28PU78	<0.2	<1.0	<0.1	--	--	<0.1	<10	37	220	2.3	1.7	95	<6.8	<1.5	160	64	Felsic dike	<
29PU78	0.5	<1.0	<0.1	--	--	<0.1	<10	39	48	16	<1.0	28	<6.8	2.7	200	73	Plagioclase porhyritic diabase	0.5
31PU78	4.7	4.0	<0.1	--	--	<0.1	<10	34	16	43	1.4	20	11	H	230	100	Fine-grained diabase dike	<
32PU78	4.7	4.0	<0.1	--	--	<0.1	<10	16	9.2	200	1.3	9.2	10	<1.5	150	76	Plagioclase porphyritic altered dike	8.7
N	1.9	3.0	<0.1	--	--	--	--	32.5	91.1	60.7	--	42.4	--	--	190	75.2		
(n)	(3)	(2)	--	--	--	--	--	(6)	(6)	(5)	--	(6)	--	--	(6)	(6)		
σ	2.4	1.4	--	--	--	--	--	9.6	112.9	79.8	--	39.0	--	--	32.3	17.2		
								GABBROIC UNIT										
1PU78	<0.2	<1.0	<0.1	--	--	<0.1	<10	41	85	74	<1.0	46	<6.8	<1.5	140	110	Metagabbro, intruded by coarse-grained hornblende gabbro	4.0
2PU78	<0.2	2.8	<0.1	--	--	<0.1	<10	25	2.1	19	<1.0	2.9	<6.8	<1.5	40	120	Metagabbro	2.8
3PU78	<0.2	<1.0	<0.1	--	--	<0.1	<10	53	10	580	<1.0	30	<6.8	<1.5	440	150	Metapyroxenite with traces of sulfide minerals	<
4PU78	<0.2	<1.0	<0.1	--	--	<0.1	<10	33	550	70	<1.0	90	<6.8	H	130	68	Metagabbro	<
13PU78	24	22	<0.1	--	--	<0.1	<10	44	140	74	2.5	39	11	H	190	130	Metagabbro interlayered with 14PU78	46
14PU78	0.4	<1.0	<0.1	--	--	<0.1	<10	32	84	12	<1.0	38	<6.8	<1.5	110	59	Metagabbro	0.4
15PU78	0.4	<1.0	<0.1	--	--	<0.1	<10	57	13	540	<1.0	23	9.1	<1.5	370	120	Gabbro with sulfide minerals	0.4
16PU78	<0.2	<1.0	<0.1	--	--	<0.1	<10	52	8.8	280	1.7	20	<6.8	<1.5	380	74	Metagabbro with traces of sulfide minerals	<
25PU78	16, 19	5.3, 15	0.1, <5	<20	100	<0.1	<1.0	35	170	32	2.6	28	<6.8	3.1	190	93	Foliated gabbro	21.3
26PU78	<0.2	2.0	<0.1	--	--	<0.1	<10	33	470	45	<1.0	92	<6.8	<1.5	82	58	Coarse-grained hornblende gabbro	2.0
43PU78	21	1.3	<0.1	<20	100	<0.1	<10	33	120	41	<1.0	18	<6.8	H	220	81	Foliated olivine-bearing gabbro	22.3
44PU78	25, 29	3.5, tr	<0.1, <5	<20	<100	<0.1	<10	44	380	7.8	3.8	29	<6.8	H	240	120	Garnet-bearing metagabbro	28.5
45PU78	14, 23	5.2, tr	0.2, <5	<20	tr	<0.1	<10	38	210	7.3	1.7	44	11	2.3	240	130	Hornblende gabbro pegmatite in metagabbro	19.4
48PU78	0.3	<1.0	<0.1	--	--	<0.1	<10	6.0	22	22	<1.0	22	8.5	0.7	27	31	Metagabbro	0.9
61PU78	3.0	7.3	0.2	<20	<100	<0.1	<10	66	750	72	<1.0	250	<6.8	<1.5	110	74	Gabbroic dikes and veins cutting dunite	10.5
62PU78	0.9	<1.0	<0.1	--	--	<0.1	<10	40	46	70	1.4	52	<6.8	<1.5	230	110	Metagabbro	0.9
67PU78	30	23	1.0	<20	<100	<0.1	<10	37	190	<32	<1.0	80	<6.8	<1.5	58	64	Metagabbro cut by muscovite-bearing granitic rock	54
70PU78	4.4	8.0	0.1	<20	140	<0.1	<10	27	83	260	<1.0	46	<6.8	<1.5	92	77	Metagabbro interlayered with metapyroxenite 71PU78	12.5
71PU78	14	24	0.6	--	--	2.6	<10	71	590	44	<1.0	280	<6.8	<1.5	87	95	Metapyroxenite interlayered with metagabbro	38.6
N	11.8	9.5	.42	<20	120	--	--	40.4	206.5	57.6	--	64.7	--	--	177.7	92.8		
(n)	(13)	(11)	(5)	--	(2)	--	--	(19)	(19)	(13)	--	(19)	--	--	(19)	(19)		
σ	10.8	8.9	.38	--	28.2	--	--	15.0	227.9	66.0	--	74.7	--	--	1,187.5	31.2		
								ULTRAMAFIC AND MAFIC CUMULATES										
7PU78	2.7	6.8	0.4	--	--	<0.1	<10	83	1,700	4.9	<1.0	1,500	<6.8	<1.5	10	64	Partially serpentinized dunite interlayered with 8PU78	9.9
8PU78	30.	33	1.3	--	--	<0.1	<10	74	1,300	58	<1.0	290	<6.8	<1.5	120	81	Wehrlite with poikilitic clinopyroxene	64.3
9PU78	8.0	11	1.1	--	--	<0.1	<10	100	1,600	4.9	<1.0	490	<6.8	<1.5	37	90	Dunite interlayered with clinopyroxenite	20.1
10PU7	48, 50	20, 45	1.7, <5	<20	<100	<0.1	<10	120	2,500	74	<1.0	2,500	9.9	<1.5	42	82	Dunite with poikilitic clinopyroxene	69.7
11PU78	18	40	18	85	250	H	<10	200	>6,800	14	<6.8	840	<6.8	<1.5	400	H	Chromitite segregations in dunite	76.
12PU78	1.7	6.8	3.9	--	--	<0.1	<10	110	>6,800	3.9	<1.0	1,400	<6.8	<1.5	90	97	do.	12.4
17PU78	1.1	<1.0	<0.1	--	--	<0.1	<10	52	760	4.2	<1.0	260	<6.8	<1.5	110	69	Clinopyroxenite with traces of olivine interlayered with gabbro	1.1

30PU78	6.1	8.5	1.2	--	--	<0.1	<10	69	1,600	3.5	<1.0	1,500	6.9	<1.5	99	80	Serpentinite slickentite intruded by diabase dikes	15.8
49PU78	8.7	11	0.4	--	--	<0.1	<10	66	1,500	6.8	<1.0	270	<6.8	<1.5	92	78	Olivine clinopyroxenite interlayered with wehrlite and dunite	20.1
51PU78	1.6	4.0	0.7	--	--	<0.1	<10	100	1,200	8.2	<1.0	450	<6.8	<1.5	14	66	Dunite interlayered with wehrlite and clinopyroxenite	6.3
52PU78	2.2	7.5	0.3	--	--	<0.1	<10	110	3,400	8.3	<1.0	1,100	7.4	<1.5	34	110	Chromitite stringers in dunite similar to 51PU78	10.0
53PU78	11	45	48	--	--	1.4	12	240	>6,800	<1.5	<1.0	590	<6.8	<1.5	<32	1,000	Chromitite layer 1 cm wide in dunite	104.0
63PU78	4.5	13	0.5	<20	tr	<0.1	<10	87	1,800	39	<1.0	1,400	<6.8	<1.5	56	92	Feldspathic peridotite dike	18
64PU78	50, 32	51, 37	1.5, <5	<20	tr	<0.1	<10	50	1,800	3.5	<1.0	190	9.1	<1.5	160	89	Clinopyroxenite interlayered with wehrlite and dunite 66PU78	102.5
66PU78	5.5	9.9	2.0	--	--	<0.1	<10	83	1,200	5.4	<1.0	500	<6.8	<1.5	17	55	Dunite interlayered with wehrlite and clinopyroxenite	17.4
72PU78	0.4	1.9	5.4	43	<100	<0.1	H	150	>21,500	4.3	3.3	1,400	<6.8	4.5	150	<15	Nodular chromitite in dunite	7.7
73PU78	0.7	3.1	8.2	35	<100	<0.1	H	170	>21,500	<1.5	<1.0	1,100	<6.8	<1.5	150	<15	Massive chromitite, layers up to 4 cm wide in dunite	12.0
74PU78	2.1	7.0	0.9	--	--	<0.1	<10	87	1,500	6.5	<1.0	940	<6.8	<1.5	9.9	80	Dunite country rock of 73PU78 and 72PU78	9.9
75PU78	9.7	3.3	0.3	--	--	<0.1	<10	45	1,400	3.1	<1.0	130	6.9	<1.5	120	<15	Clinopyroxenite interlayered with dunite	13.3
76PU78	16	41	2.0	--	--	<0.1	<10	50	1,600	5.1	<1.0	190	<6.8	<1.5	84	83	Wehrlite interlayered with clinopyroxenite 75PU78	59.
77PU78	1.6	27	5.8	29	<100	H	<10	140	>21,500	4.0	<1.0	1,700	<6.8	4.5	100	<15	Chromitite layers in dunite	50.1
78PU78	3.7	4.9	1.3	--	--	<0.1	<10	80	1,500	6.5	<1.0	1,600	<6.8	<1.5	7.9	61	Dunite interlayered with clinopyroxenite 79PU78	9.9
79PU78	6.1	7.7	1.1	--	--	<0.1	<10	70	1,600	<32	<1.0	1,700	<6.8	<1.5	37	59	Clinopyroxenite interlayered with dunite	15.1
N	10.3	13.3	3.0	48.0	<250	--	--	101.6	1,644.7	13.4	--	958.3	--	--	88.2	129.8		
(n)	(20)	(18)	(18)	(4)	(1)	--	--	(23)	(17)	(20)	--	(23)	--	--	(22)	(18)		
σ	15.0	13.9	4.3	25.3	--	--	--	49.8	575.1	19.8	--	647.2	--	--	85.5	217.7		
TECTONITE AND ASSOCIATED DIKES																		
18PU78	5.3	6.1	0.5	--	--	<0.1	<10	89	1,500	47	<1.0	2,200	<6.8	<1.5	22	73	Harzburgite with tectonite fabric	11.9
19PU78	10	19	3.0	--	--	<0.1	<10	93	2,000	4.6	<1.0	2,200	<6.8	<1.5	14	77	Dunite with tectonite fabric interlayered with 19PU78	32.0
20PU78	0.5	<1.0	2.1	--	--	<0.1	<10	81	2,100	3.3	<1.0	1,800	<6.8	<1.5	7.8	43	Coarse-grained chromitite in dunite pod	2.6
21PU78	6.4	5.3	<0.1	--	--	<0.1	<10	35	1,800	7.3	<1.0	420	<6.8	<1.5	100	64	Chrome spinel and diopside vein cutting orthopyroxenite	11.7
23PU78	0.5	4.7	1.6	29	<100	<0.1	<10	140	>6,800	10	<1.0	1,900	<6.8	H	120	H	Chromitite float	6.8
24PU78	1.1	5.3	2.7	38	<100	H	<10	150	6,800	14	<1.0	2,000	<6.8	<1.5	100	280	Chromitite float from same area as 23PU78	9.1
34PU78	17	9.5	0.2	--	--	<0.1	<10	110	3,400	73	<1.0	2,500	<6.8	<1.5	28	100	Crosscutting dunite, partially serpentinize	26.7
36PU78	2.5	4.7	1.0	--	--	<0.1	<10	94	780	4.8	<1.0	2,500	7.6	<1.5	12	61	Croscutting dunite with chromite	8.2
37PU78	2.2	9.2	0.3	<20	tr	<0.1	<10	61	3,600	230	<1.0	1,500	<6.8	H	120	62	Wehrlite dike cutting harzburgite	11.7
38PU78	2.3	8.0	1.4	--	--	<0.1	<10	110	1,200	4.2	<1.0	2,500	<6.8	<1.5	11	68	Crosscutting serpentinized dunite	11.7
39PU78	3.0	10	1.1	--	--	<0.1	<10	97	1,800	8.8	<1.0	2,400	<6.8	<1.5	30	71	Harzburgite with tectonite fabric	14.1
40PU78	7.0	9.9	1.4	--	--	<0.1	<10	93	1,500	2.7	<1.0	2,100	<6.8	<1.5	25	67	Harzburgite cut by crosscutting dunite	19.3
41PU78	1.5	9.0	0.8	<20	<100	H	<10	150	>6,800	31	2.1	1,700	<6.8	H	100	H	Chromitite	11.2
42PU78	4.1	17	4.4	31	170	<0.1	<10	160	>6,800	31	<1.0	1,800	<6.8	<1.5	120	470	Chromitite in dunite	25.5
46PU78	6.5	7.7	0.7	--	--	<0.1	<10	90	1,300	18	<1.0	1,700	<6.8	<1.5	22	87	Harzburgite cut by dike of 47PU78	14.9
47PU78	1.4	2.9	<0.1	<20	tr	<0.1	<10	76	1,200	12	<1.0	370	<6.8	<1.5	110	100	Clinopyroxenite with minor olivine as a dike	4.3
54PU78	6.5	7.3	1.0	--	--	<0.1	<10	96	1,900	14	<1.0	2,000	7.7	<1.5	37	82	Antigorite-olivine schist in shear zone	14.8
55PU78	4.0	5.5	0.5	--	--	<0.1	<10	130	3,900	2.6	<1.0	2,400	<6.8	<1.5	27	110	Disseminated and lense-shape chromitite in antigorite serpentinite	10.
56PU78	0.9	<1.0	0.1	31	<100	0.69	<10	140	>6,800	3.6	<1.0	2,300	<6.8	4.0	140	<15	Disseminated chromitite	1.0
57PU78	0.4	2.1	4.6	<20	100	<0.1	<10	100	1,600	4.2	<1.0	2,400	7.9	<1.5	35	69	Harzburgite tectonite	7.1
58PU78	4.0	6.8	0.5	54, 38	240, 190	<0.1	<10	160	>21,500	<1.5	<1.0	1,500	<6.8	<1.5	<32	<15	Massive and nodular chromitite	11.3
59PU78	1.9	3.3	0.3	<20	140	<0.1	<10	100	3,300	6.3	<1.0	2,400	<6.8	<1.5	34	88	Stream sediment from basin containing 57 and 58PU78	5.5
60PU78	1.7	2.1	5.7	<20	<100	<0.1	<10	110	2,500	3.1	<1.0	1,100	11	<1.5	17	82	Dunite	9.5
N	3.9	7.5	1.7	36.8	185	--	--	106.7	2,081.2	24.3	--	1,899.6	--	--	56.0	103.9		
(n)	(2)	(19)	(19)	(6)	(4)	--	--	(23)	(17)	(22)	--	(23)	--	--	(22)	(19)		
σ	3.9	4.4	1.7	9.2	42.0	--	--	31.4	934.6	49.1	--	605.7	--	--	46.0	94.4		

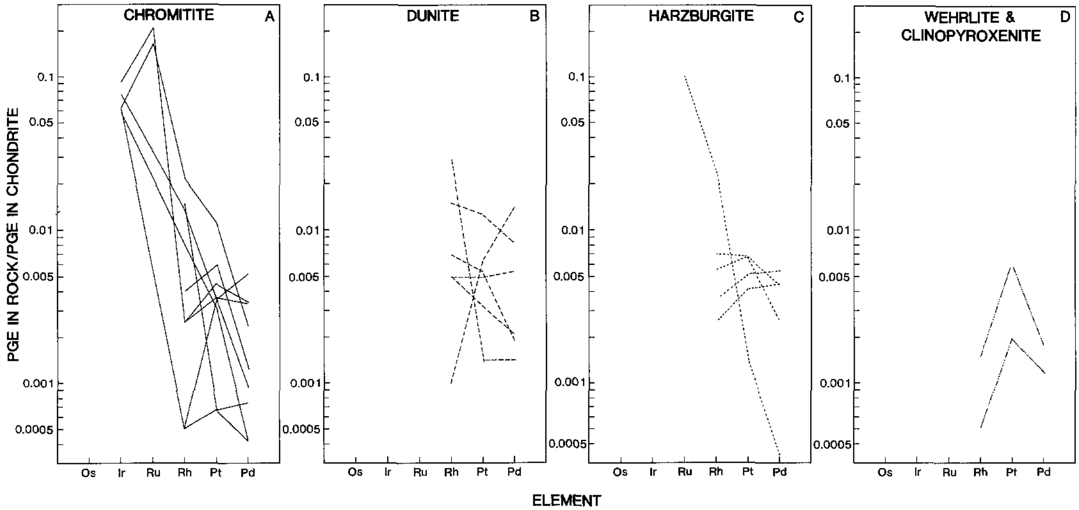

Fig. 2. Chondrite-normalized PGE ratios for individual rock samples from the ultramafic tectonite unit. A. Chromitite. B. Dunite. C. Harzburgite. D. Wehrlite and clinopyroxenite

the chondrite normalized ratios for Pd, Pt, and Rh have essentially the same value, (2) hump-shaped patterns, that is the chondrite normalized ratio for Pt is larger than that for Pd or Rh, (3) positively sloping patterns, and (4) negatively sloping patterns. Within the tectonite unit (Fig. 2), the chondrite normalized patterns for individual rocks are either approximately flat or negatively sloping except for wehrlite, clinopyroxenite, and dunite-orthopyroxenite dikes. Samples from interlayered dunite and harzburgite tectonite yield approximately flat patterns; negatively sloping patterns are most common from samples of chromitite, harzburgite with abundant chromite, and cross-cutting dunites containing chromite. In general, within the ultramafic and mafic cumulate unit (Fig. 3), samples of chromitite display negatively sloped patterns, and interlayered dunite, wehrlite, and clinopyroxenite show positively sloping patterns, with a few exceptions of both flat and hump-shaped patterns shown by various rock types. Chondrite normalized patterns for individual samples of the gabbroic unit (Fig. 4) are more difficult to characterize because of the large portion of less than detectable contents of PGE in a number of samples (Table 1). If the "less-than" contents are treated as maximum chondrite normalized ratios, then hump-shaped, positively and negatively sloping patterns are shown by individual gabbroic rocks.

Average concentrations for the units in the ophiolite (Table 2) yield negatively sloping chondrite normalized patterns (Fig. 5). The patterns for ultramafic tectonite and associated dikes, ultramafic and mafic cumulates, and the chromitites have negative slopes and show more depletion in platinum and palladium than in iridium and ruthenium compared to chondrites. These patterns are similar to those obtained for chromitites in tectonite and from near the base of the cumulates in the Samail ophiolite, Oman (Page and others, 1979). The gabbroic unit of the Voikar-Syninsky ophiolite complex appears to have a different pattern from the rest of the ophiolite. Although the patterns of chondrite-normalized Ir, Ru, and Rh for the gabbroic unit are similar to those of other units, the pattern of Pt and Pd are quite different. The positive trend for the Rh, Pt, and Pd end of this pattern is similar to those obtained from stratiform cumulate sequences (Page, von Gruenewaldt, Aruseavage,

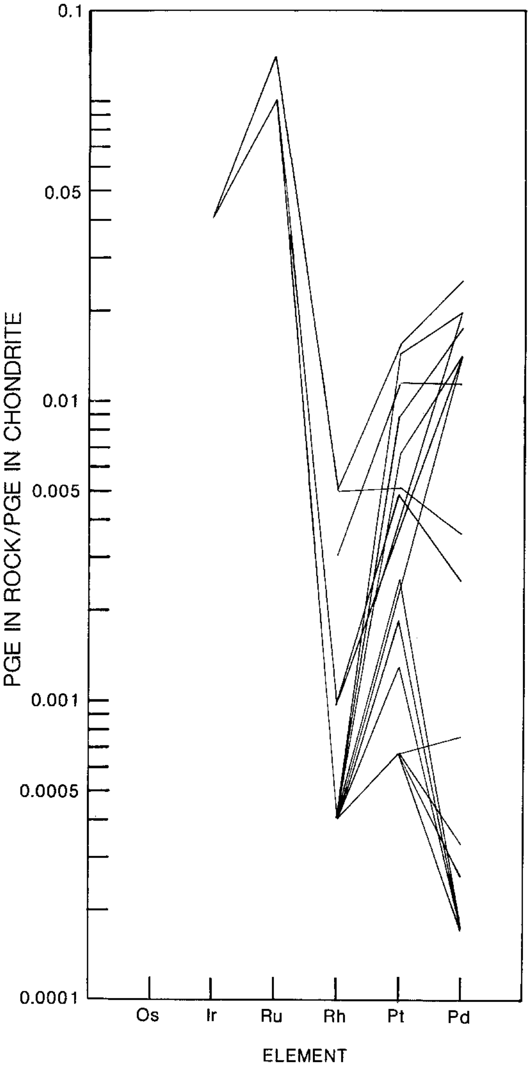

Fig. 3. Chondrite-normalized PGE ratios for individual rock samples from the ultramafic and mafic cumulate unit

and Haffty, 1982). The simplification (Fig. 6) of the patterns of chondrite normalizd PGE ratios from Figures 2, 3, and 4 is composed of areas containing the four most common patterns and compares these areas with the area within which chondrite normalizd PGE ratios of ultramafic xenoliths from basalts and kimberlites occur based on the data of Morgan and Wandless (1979), Jagoutz and others (1979), and Morgan and others (1980). Most of the xenoliths have been analyzed for Os, Ir, Pd, and less frequently for Pt, but the chondrite normalized ratios for these elements form approximately flat patterns within the area A of Figure 6. Some of the analyzed xenoliths have been assumed to represent undepleted pristine mantle. Comparison of chondrite-normalized patterns of xenoliths with those from the Voikar-Syninsky ophiolite suggest that the approximately flat patterns originating

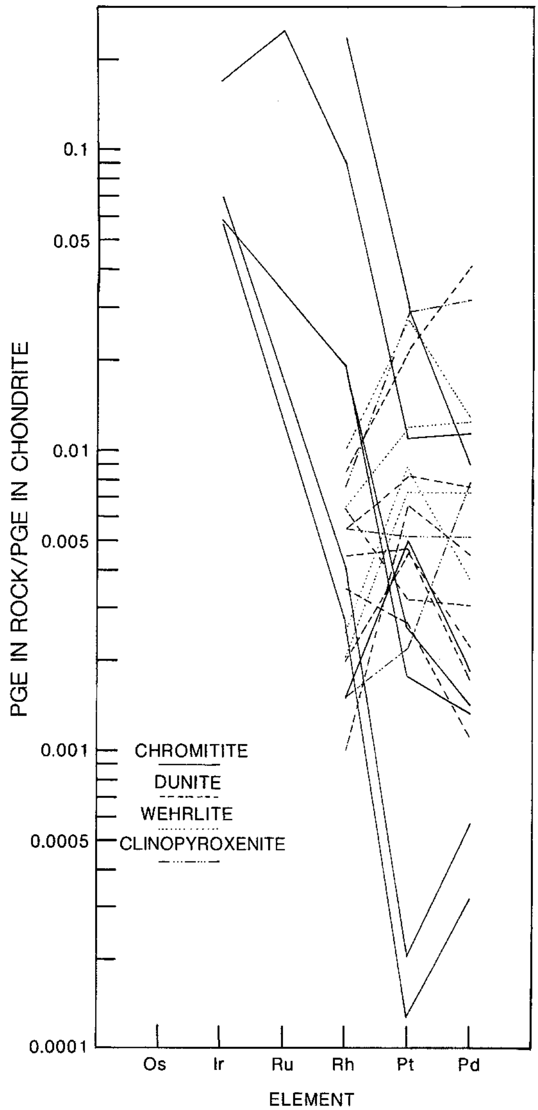

Fig. 4. Chondrite-normalized PGE ratios for individual rock samples from the gabbroic unit

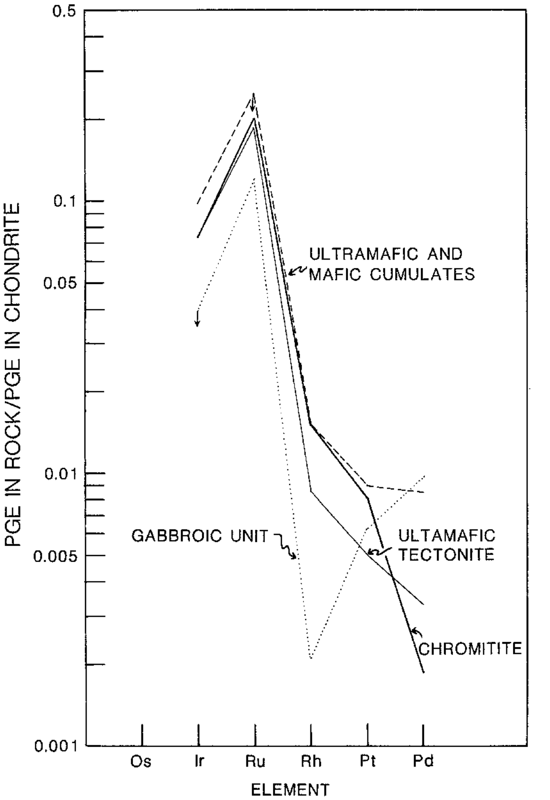

Fig. 5. Chondrite-normalized PGE ratios for the ultramafic tectonite, ultramafic and mafic cumulates, gabbroic, and dike complex units of the Voikar-Syninsky ophiolite complex. Arrows indicate maximum ratios

from dunite and harzburgite tectonites, area B in Figure 6, may also represent undepleted mantle with respect to the PGE. The negatively sloping chondrite normalized PGE patterns derived from mainly chromitites occur in area C. Such patterns represent an enrichment of Ir and Ru and depletion in Pt and Pd with respect to ultramafic xenoliths. If the chromitite represents the early formed crystallization products from a magma passing through the lower part of the ophiolite in a manner similar to that proposed by Cassard and others (1981), then the enrichment relative to xenoliths of Ir and Ru and potentially Os could be due to the crystallization of Os-Ir-Ru alloys or sulfides at high temperatures that were trapped as inclusions in the chromite crystals, whereas the depletion in the chromitites of Pt and Pd might reflect that these elements remained concentrated in the magma that escaped from the immediate system. Minerals containing Os, Ir, and Ru have been identified within chromitite from other ophiolite complexes (Constantinides and others, 1980; Z. Johan, written commun., 1980; H. Stockman, oral commun., 1980). The positively sloping patterns of chondrite normalized ratios of interlayered dunite,

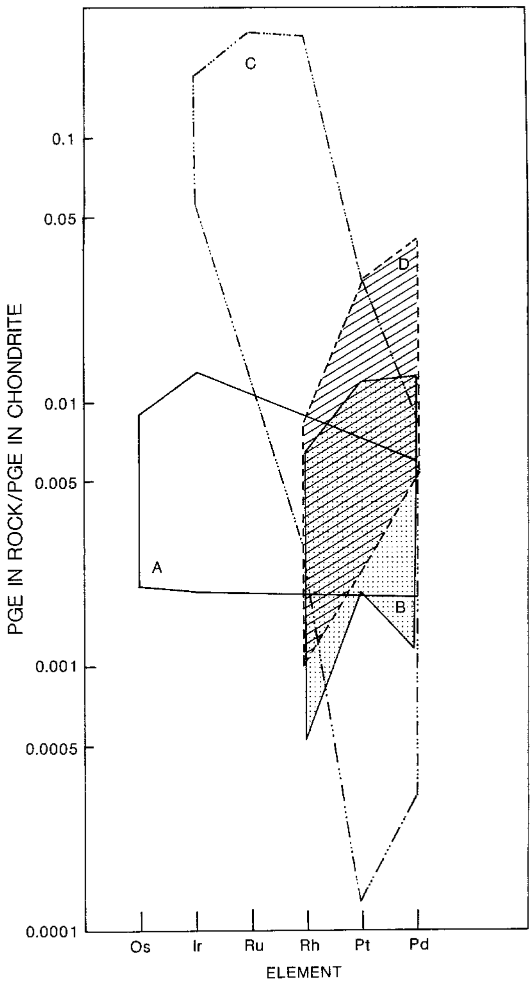

Fig. 6. Cartoon-like plot of chondrite-normalized PGE patterns as areas for each characteristic pattern, discussed in the text

wehrlite, and clinopyroxenite of the ultramafic and mafic cumulate unit fall in area D of Fig. 6, as do some of the patterns from the gabbroic unit. An enrichment in Pt and Pd with respect to ultramafic xenoliths is indicated by this pattern and might be the result of concentration of Pt and Pd in an immiscible sulfide melt that could accumulate in these rocks.

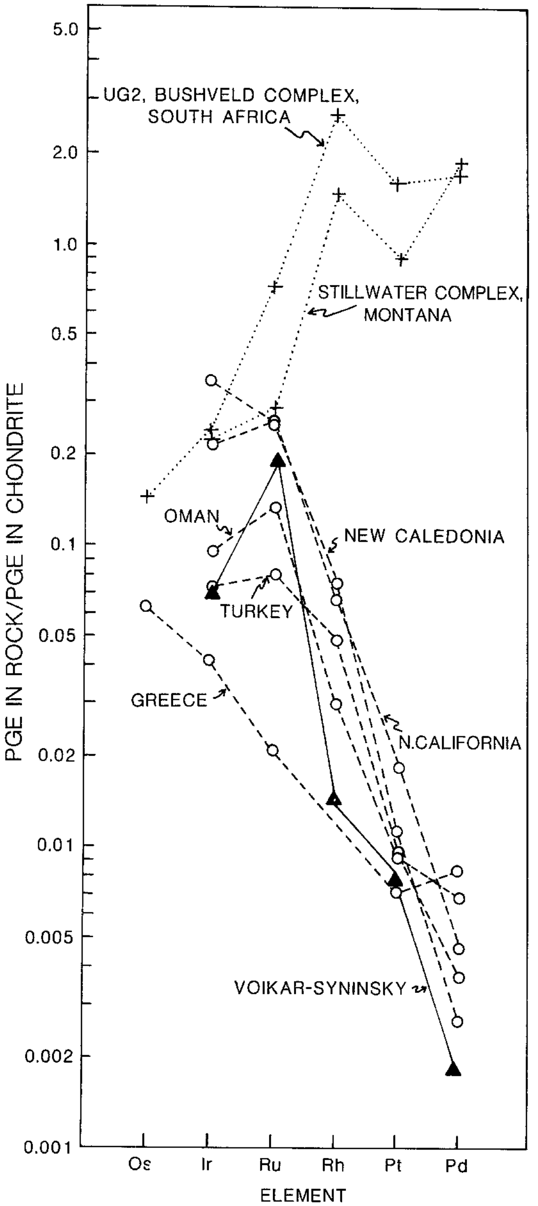

Fig. 7. Comparison of chondrite-normalized PGE patterns of chromitite in ophiolite and stratiform complexes with the pattern for chromitite from the Voikar-Syninsky ophiolite complex

COMPARISON OF PGE DATA WITH OTHER OPHIOLITES

Studies by Page, Pallister and others (1979) on the Samail ophiolite, Oman; Page, Cassard, and Haffty (1982) on the Massif du Sud and Tiebaghi Massif ophiolites, New Caledonia; Page, Haffty, Ahmad (1980) on ophiolites in Pakistan and Page, Engin, and Haffty (1980) on ophiolites in Turkey have established that chondrite-normalized PGE in chromitites from these Mesozoic ophiolites have negatively sloping patterns when plotted (Fig. 7). The chromitites from the Voikar-Syninsky ophiolite have a similar pattern. Thus, all ophiolite-associated chromitites so far examined have patterns with slopes opposite to those shown by chromitites in stratiform complexes.

If magmas that form both chromitite in both ophiolites and stratiform complexes originate from mantle material with similar PGE concentrations and ratios, then the processes, either partial melting of mantle material, concentration within the complexes, or both, involved are different, which is the hypothesis favored in this report. It is most likely that PGE patterns represent the percentage or portion of mantle material melted to produce the original melts. However, if the normalized PGE patterns represent source materials that are different, it should be possible, by examining chondrite-normalized PGE patterns, to map mantle compositions as characterized by PGE contents.

CONCLUSIONS

The PGE geochemistry and chondrite-normalized PGE patterns of chromitites in Paleozoic and Mesozoic ophiolite complexes are similar, suggesting that chondrite-normalized PGE patterns may be used to identify ophiolites where they occur in a highly dismembered manner. The gabbroic unit of the Voikar-Syninsky ophiolite appears to have a different PGE geochemistry from the tectonite and ultramafic and mafic cumulate units, possibly suggesting that they differentiated and accumulated by processes similar to those by which gabbroic rocks in stratiform complexes form.

REFERENCES

Bogdanov, N.A., Morgan, B.A., Page, N.J: Ophiolite complex traversed. Geotimes, February 1979, 22-23 (1979)

Cassard, D., Nicolas, A., Rabinovitch, M., Moutte, J., Leblanc, M., Prinzhofer, A.: Structural classification of chromite pods in southern New Caldonia: Economic Geology, v. 76, 805-831 (1981)

Constantinides, C.C., Kingston, G.A., Fisher, P.C.: The occurrence of platinum group minerals in the chromitides of the Kokkinorotsos chrome mine, Cyprus. In: Ophiolite, proceedings international ophiolite symposium 1979. Geological Survey Department, Cyprus Ministry of Agriculture and Natural Resouces, Printco, Nicosia, Cyprus, p 93-101, 1980

Efimov, A.A., Lennykh, V.I., Puchkov, V.N., Savelyev, A.A., Savelyeva, G.N., Jaseva, R.G.: Guidebook for excursion, ophiolites of Polar Urals. In: Bogdanov N.A. (ed.) 4th field conference. Moscow, August 1-15, 1978

Haffty, Joseph, Riley, L.B.: Determination of palladium, platinum, and rhodium in geologic materials by fire assay and emission spectrography. Talanta 15, 111-117 (1968)

Haffty, Joseph, Riley, L.B., Goss, W.D.: A manual on fire assaying and determination of the noble metals in geological materials. U.S. Geological Survey Bulletin 1445, 58 (1977)

Haffty, Joseph, Haubert, A.W., Page, N.J: Determination of iridium and ruthenium in geological samples by fire assay and emission spectrography. U.S. Geological Survey Professional Paper 1129-G, G1-G4 (1980)

Jagoutz, E., Palme, H., Baddenhausen, H., Blum, K., Cendales, M., Dreibus, G., Spettel, B., Lorenz, W., Wanke, H.: The abundances of major, minor, and trace elements in the earth's mantle as derived from primitive ultramafic nodules, Lunar and Planetary Science, 10, 610-612 (1979)

Knipper, A.: Ophiolite belt of the Urals, IGCP Project "Ophiolites", International Atlas of ophiolites. Geological Society of America Map and Chart Series MC-33 sheet 3, scale 1:2,500,000 (1979)

McBryde, W.A.E.: Platinum metals. In: Fairbride, R.W. (ed.) The encyclopedia of geochemical and environmental sciences. New York, Van Nostrand Reinhold Co, 1972

Morgan, J.W., Wandless, G.A.: Terrestrial upper mantle: Siderophile and volatile trace element abundances: Lunar and Planetary Sciencė, 10, 855-857 (1979)

Morgan, J.W., Wandless, G.A., Petrie, R.K., Irving, A.J.: Earth's upper mantle: volatile element distribution and origin of siderophile element content: Lunar and Planetary Science, 11, 740-742 (1980)

Page, N.J, Engin,T., Haffty, J.: Palladium, platinum, and rhodium concentrations in mafic and ultramafic rocks from the Kizildag and Guleman areas, Turkey, and the Faryab and Esfandagheh-Abdasht areas, Iran. U.S. Geological Survey Open-File Report 79-840, 15 (1980)

Page, N.J, Haffty, J., Ahmad, Z.: Palladium, platinum, and rhodium concentrations in mafic and ultramafic rocks from the Zhob Valley and Dargai Complexes, Pakistan. In: Shorter contributions to mineralogy and petrology, 1979. U.S. Geological Survey Professional Paper 1124-F, F1-F6 (1980)

Page, N.J, Myers, J.S., Haffty, J., Simon, F.O., Aruscavage, P.J.: Platinum, palladium, and rhodium in the Fiskenaesset Complex, southwestern Greenland. Economic Geology, 75, 907-915 (1980)

Page, N.J, Pallister, J.S., Brown, M.A., Smewing, J.P., Haffty, J.: Comparison of the distribution of platinum-group metals in chromiterich rocks from two traverses through the Semail Ophiolite, Oman, (Abs.). Fall AGU meetings Abs. Dec 3-7, 1979

Page, N.J, Cassard, D., Haffty, J.: Palladium, platinum, rhodium, ruthenium, and iridium in chromitites from the Massif du Sud and Tiebaghi Massif, New Caledonia, Economic Geology 77, 1571-1577 (1982)

Page, N.J, Gruenewaldt, G., Haffty, J.,, Aruscavage, P.J.: Comparison of platinum, palladium, and rhodium distributions in some layered intrusions with special reference to the late differentiates (upper zones) of the Bushveld Complex, South Africa. Economic Geology 77, 1405-1418 (1982)

Savelyev, A.A., Savelyeva, G.N.: Ophiolites of the Voikaro-Sinsky massif (Polar Urals). Geotectonics 6, 46-60 (1977)

Savelyeva, G.N., Stephanov, S.S.: Evolution of eustatite during high-temperature deformations of harzburgites of the Vokar-Syn'ya Massif (Polar Urals). International Geology Review 22, 270-278 (1980)

Simon, F.O., Aruscavage, P.J., Moore, R.: Determination of platinum, palladium, and rhodium in geologic spectroscopy using electrothermal atomization. American Chemical Society, 176th National Meeting, September 11-014, 1978, Miami Beach, Fla.(1978)

Sobolev, F.J., Dobretsov, N.L.: Petrology and metamorphism of ancient ophiolites - An example of the Polar Urals and West Sayan. Siberian Branch of the Academy of Sciences in Transactions of the Institute of Geology and Geophysics Issue 368, 217 (1977)

Received: June 15, 1982

N.J Page
U.S. Department of the Interior
Geological Survey, Branch of Western Mineral Resources
345 Middlefield Road MS-41
Menlo Park, Ca, 94025
USA